Journal of Magnetism and Magnetic Materials 104–107 (1992) 737–738
North-Holland

Magnetocrystalline anisotropy of $RECo_5$ compounds

G.H.O. Daalderop, P.J. Kelly and M.F.H. Schuurmans

Philips Research Laboratories, 5600 JA Eindhoven, Netherlands

The magnetocrystalline anisotropy energy and anisotropy of the orbital angular momentum have been calculated ab initio for YCo_5 using the LMTO method. Quantitative agreement with experiment is found if a recently proposed *orbital polarization* correction is included. The anisotropy of the orbital angular momentum and the energy are strongly correlated. The crystal field parameters at the RE site in $RECo_5$ compounds, calculated using the FLAPW method, have the correct sign and are comparable to the experimentally observed values.

The compound $SmCo_5$ is of considerable interest because of its large magnetocrystalline anisotropy energy (MAE) of 0.016 eV/unit cell [1–3]. This anisotropy is in large part due to single ion anisotropy originating from rare earth (RE) 4f electrons localized on the RE site which has hexagonal symmetry. However, because the anisotropy energy of YCo_5 is only a factor of four smaller [4], itinerant Co 3d electrons are also believed to contribute substantially to the anisotropy energy. In this paper we present for $RECo_5$ compounds *first principles* calculations of the anisotropy within the framework of the local-spin-density-approximation (LSDA) [5].

The anisotropy energy of YCo_5 is obtained by first solving the Kohn–Sham equations [5] self-consistently for the scalar-relativistic spin polarized Hamiltonian for the material with n valence electrons. This is done using the linear muffin tin orbital (LMTO) method in the atomic sphere approximation (ASA) including s, p, d and f partial waves in the basis [6]. The spin–orbit coupling term, $\xi \boldsymbol{l} \cdot \boldsymbol{\sigma}$, is then added and the full Hamiltonian is diagonalized for two directions of the magnetization. The force theorem is used to calculate the anisotropy energy, $\Delta E = E(\hat{\boldsymbol{n}} \parallel \boldsymbol{c}) - E(\hat{\boldsymbol{n}} \perp \boldsymbol{c})$, as the difference in sums of Kohn–Sham eigenvalues [7]. $E(\hat{\boldsymbol{n}})$ is the total energy when the magnetization is oriented in the direction $\hat{\boldsymbol{n}}$. The anisotropy in the orbital angular momentum is defined analogously. We have also investigated the influence on the MAE of an orbital polarization correction, recently proposed [8] to take account of Hund's second rule. The orbital polarization term in the Hamiltonian has the form $-BL\boldsymbol{l} \cdot \hat{\boldsymbol{n}}$, where the Racah B parameter is calculated using the radial d wavefunctions. The orbital angular momentum, L, is obtained by iterating the relativistic Hamiltonian (including both spin–orbit coupling and orbital polarization) to self-consistency with $\hat{\boldsymbol{n}} \parallel \boldsymbol{c}$. The MAE is then calculated using the force theorem. By calculating the anisotropy energy – denoted $\Delta E^n(q)$ – as a function of the bandfilling q, it is shown to be strongly correlated with the anisotropy in the orbital angular momentum, $\Delta L^n(q)$.

In fig. 1(a) the anisotropy energy versus bandfilling is shown by the solid line, obtained including spin–orbit coupling together with orbital polarization; the dotted line indicates results obtained including spin–orbit coupling only. The correct easy axis is predicted and good quantitative agreement with experiment is obtained if orbital polarization is included. The anisotropy in the orbital angular momentum (shown as the dashed

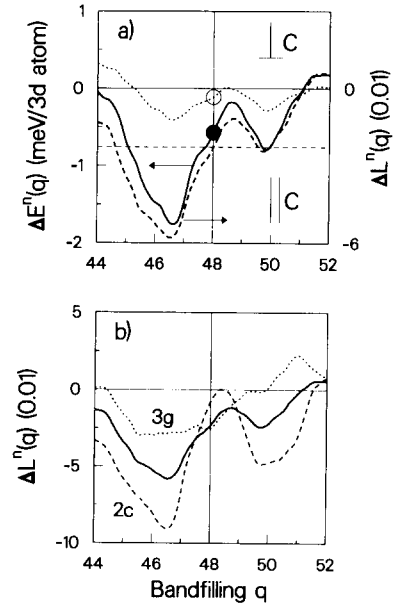

Fig. 1. (a) The magnetic anisotropy energy per 3d atom, $\Delta E^n(q)$, versus bandfilling q (solid: calculation including spin–orbit coupling together with orbital polarization, dotted curve: spin–orbit coupling only). The anisotropy of the orbital angular momentum per 3d atom (calculated including orbital polarization) is shown by the dashed curve, referred to the right-hand axis. The actual number of valence electrons, n, is denoted by the vertical line, and the experimental anisotropy energy is indicated by the horizontal dashed line. (b) The anisotropy in the orbital angular momentum per Co atom at the 2c site (dashed) and 3g site (dotted), in units of $\hbar$, and the average anisotropy per Co atom (solid).

curve in fig. 1(a)) is clearly correlated with the anisotropy energy. In fig. 1(b) the anisotropy in the orbital angular momentum is resolved into contributions from the Co atoms at the two different types of sites in this structure, the 2c and 3g sites. The peaked structure is seen to be mainly determined by the Co_{2c} atoms. Although there were experimental indications that the anisotropy was to be associated with these types of atoms [4], we find that at the actual Fermi energy ΔL_{3g} exceeds ΔL_{2c}.

Within the minority spin subband, orbital polarization represents an effective spin–orbit coupling parameter $\bar{\xi} = \xi + BL$. Within perturbation theory [9] the orbital angular momentum is proportional to ξ, and in the limit of large exchange splitting a new orbital angular momentum of $L = L_0/(1 - L_0 B/\xi)$ results upon including orbital polarization, where L_0 is the orbital angular momentum obtained without orbital polarization. At the center of the occupied minority spin d bands, $\xi = 33$ meV and $B/\xi = 3.9$. The increase in the orbital angular momentum, from $L_0 = 0.12$ to $L = 0.23\hbar$ for each Co atom, is well described by this relation. With the same approximations, the energy gain upon including the spin–orbit coupling and orbital polarization, $E^n(q, \hat{n}) - E^n_{\xi=0}(q)$, is given by $\frac{1}{2}\bar{\xi}L^n(q, \hat{n})$. It can be seen in fig. 1(a) that the ratio $\Delta E^n(q)/\Delta L^n(q)$ is given well by the proportionality factor $\frac{1}{2}\bar{\xi}$. When orbital polarization is included, the spin magnetic moments of the Y, Co_{2c} and Co_{3g} atoms are -0.32, 1.33 and $1.51\mu_B$ respectively, resulting in a total (spin and orbital) calculated magnetic moment of $1.60\mu_B$ per Co atom, compared to the experimental value of $1.66\mu_B$ [4]. The discrepancy in the calculated magnetic moment with respect to the experimental value is comparable to the discrepancy of $0.05\mu_B$ obtained for hcp Co.

Within the approximation that the interaction between the 4f electrons and the valence electrons may be treated perturbatively, crystal field parameters may be calculated straightforwardly within the framework of the LSDA. We expand the Hartree potential within a muffin tin sphere on the RE site, $v(r)$, in Cartesian functions t_l^m of degree l (corresponding to Tesseral Harmonics apart from a prefactor) [10]; $v(r) = \sum_{l,m} w_l^m(r) t_l^m(\hat{r})$. The crystal field parameters, A_l^m, are then given by $A_l^m\langle r^l\rangle = -e\int R_{4f}^2(r) w_l^m(r) r^2 dr$, where $w_l^m(r)$ describes the radial dependence of the potential, R_{4f} is the radial 4f wavefunction and $\langle r^l\rangle = \int R_{4f}^2(r) r^{l+2} dr$. Because the crystal field parameters are not found to vary strongly with the type of RE atom [3], we calculate $A_l^m\langle r^l\rangle$ for $GdCo_5$; with a half filled f shell the Gd 4f charge density is spherically symmetric and the 4f states may be treated as core-like states in the LSDA calculations. The non-spherical valence charge density is obtained from self-consistent calculations with the full potential linear augmented plane wave (FLAPW) method [11,6].

Table 1
Crystal field parameters A_l^m times radial expectation values $\langle r^l\rangle$ in $GdCo_5$ separated into on-site and lattice contributions in K. The calculated radial expectation values are $\langle r^2\rangle = 0.93a_0^2$ and $\langle r^4\rangle = 2.11a_0^4$

	On-site		Lattice	Total	Expt.
$A_2^0\langle r^2\rangle$		−1743	980	−763	−180[1]; −420[2]; −210[3]
	5p–5p	87			
	6p–6p	−407			
	5d–5d	−775			
	others	−648			
$A_4^0\langle r^4\rangle$		−3	−24	−27	–

The resulting values for $A_l^m\langle r^l\rangle$ are given in table 1, divided into on-site and lattice contributions, based upon the separation of $w_l^m(r)$ into these contributions [12]. The 5p states are found to contribute only −15% to A_2^0. About 44 and 23% respectively of the on-site contribution to A_2^0 can be attributed to d–d and p–p contributions from the wavefunctions to the charge density [13]. Whereas the lattice contribution to A_2^0 is comparable to the on-site contribution, it completely dominates A_4^0.

We conclude that the itinerant electron contribution to the magnetocrystalline anisotropy and the crystal field parameters can be calculated from *first principles*.

References

[1] K.H.J. Buschow, A.M. van Diepen and H.W. de Wijn, Solid State Commun. 15 (1974) 903.
[2] S.G. Sankar et al., Phys. Rev. B 11 (1975) 435.
[3] R.J. Radwański, J. Magn. Magn. Mater. 62 (1986) 120.
[4] J.M. Alameda et al., J. Appl. Phys. 52 (1981) 2079. J. Déportes et al., IEEE Trans. Magn. MAG-12 (1976) 1000.
[5] O. Gunnarsson and R.O. Jones, Rev. Mod. Phys. 61 (1989) 689 and references therein.
[6] O.K. Andersen, Phys. Rev. B 12 (1975) 3060.
[7] G.H.O. Daalderop, P.J. Kelly and M.F.H. Schuurmans, Phys. Rev. B 41 (1990) 11919 and references therein.
[8] M.S.S. Brooks, Physica B 130 (1985) 6. O. Eriksson et al., Phys. Rev. B 42 (1990) 2707.
[9] J. Friedel, in: The Physics of Metals, ed. J.M. Ziman (Cambridge Univ. Press, Cambridge, 1969). P. Bruno, Phys. Rev. B 39 (1989) 865.
[10] M.T. Hutchings, in: Solid State Physics, vol. 16, eds. F. Seitz and D. Turnbull (Academic Press, New York, 1964). p. 227.
[11] H.J.F. Jansen and A.J. Freeman, Phys. Rev. B 30 (1984) 561.
[12] M. Weinert, J. Math. Phys. 22 (1981) 2433.
[13] R. Coehoorn and G.H.O. Daalderop, J. Magn. Magn. Mater. 104–107 (1992) 1081, and references therein.